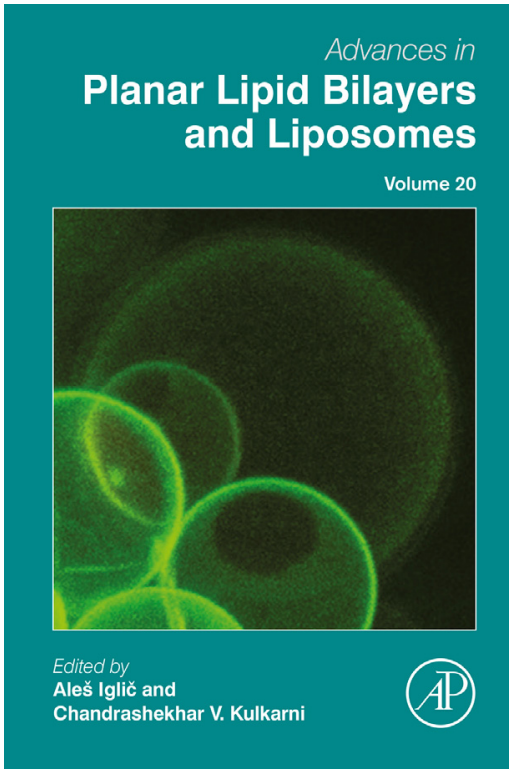

From: Natalia Wilke, Lipid Monolayers at the Air–Water Interface: A Tool for Understanding Electrostatic Interactions and Rheology in Biomembranes. In Aleš Iglič, Chandrashekhar V.Kulkarni editors: *Advances in Planar Lipid Bilayers and Liposomes*, Vol. 20,
Burlington: Academic Press, 2014, pp. 51-81.
ISBN: 978-0-12-418698-9

CHAPTER TWO

Lipid Monolayers at the Air–Water Interface: A Tool for Understanding Electrostatic Interactions and Rheology in Biomembranes

Natalia Wilke[1]

Centro de Investigaciones en Química Biológica de Córdoba (CIQUIBIC), Dpto. de Química Biológica, Facultad de Ciencias Químicas, Universidad Nacional de Córdoba, Pabellón Argentina, Ciudad Universitaria, X5000HUA Córdoba, Argentina

[1]Corresponding author: e-mail address: wilke@mail.fcq.unc.edu.ar; natiwilke@gmail.com

Contents

Abstract

Monomolecular films of surfactants at the air–water interface are easy to prepare and handle, and enable a broad variety of techniques to be used. As in other model systems mimicking membranes, two phases are observed in several experimental conditions. This chapter compares the results found using this model membrane with other models and describes some of the techniques applicable to lipid monolayers. The factors underlying their texture when two phases coexist are summarized, with special attention to line tension, an important parameter in both nucleation and growth, as well as the final domain shape. Finally, the effects of the presence of two phases on the observed mechanical properties of the film (elastic compressibility and shear viscosity) are detailed.

Advances in Planar Lipid Bilayers and Liposomes, Volume 20
ISSN 1554-4516
http://dx.doi.org/10.1016/B978-0-12-418698-9.00002-2

1. INTRODUCTION

When amphiphiles are dissolved in an organic solvent and deposited on a water surface, the solution spreads rapidly to occupy the available area. While the solvent evaporates, the surfactant orientates to minimize contact of its nonpolar regions with water, but maximizes the water contact of its polar region, resulting in a one-molecule-thick surfactant film named "Langmuir monolayer." These self-structured thin films have been the subject of study for many decades from a fundamental point of view in the fields of biophysics and biology as model biomembranes [1–7] and also as bottom-up 2D-patterning of molecularly thin films for different uses [8–14].

Langmuir monolayers are extremely valuable models for membranes [2,6,7,15,16] since experiments can easily be performed in which the molecular area, surface pressure, temperature, and chemical nature of the subphase are varied, and by this means, a broad set of thermodynamic parameters that characterize the monolayer can be accurately determined [1,17,18]. Although transmembrane processes cannot be studied in monolayers, this system is well suited for studying lateral mixing and structuring mediated by a variety of lipids and proteins which constitute biomembranes [5,19–23]. Using this model membrane, a broad spectrum of techniques can be applied, some of which are detailed in Section 2. These lipid films also enable the diffusing species to be followed over a relatively large area and for a long time. Furthermore, the environment of such molecules can be controlled and also varied in a controlled manner (see Section 5).

All of this makes Langmuir lipid monolayers a convenient system for analyzing the influence of domains on the mechanical properties of membranes. The results found using Langmuir monolayers and other model membranes are similar in some cases but not in others, raising the interesting question of which model system is more suitable, the answer to which may depend on the parameter under study (see Section 6).

2. EXPERIMENTAL APPROACHES ON MONOLAYERS

Once Langmuir monolayers are formed, these films can be compressed while the area of the interface and the surface tension are determined, which is usually performed using a Wilhelmy plate made of platinum or paper. The surface pressure "π" can then be calculated as the surface tension of the bare interface minus that of the interface modified

by the lipid layer, with the plots of π as a function of the mean molecular area "MMA" (interface area divided by the number of molecules at the interface) being referred to as "compression isotherms." These experiments have been detailed elsewhere (see, e.g., Refs. [1,4,6]). For most lipid monolayers, the slope of the compression isotherm indicates the film's response under expansion or compression since shear can be neglected [24]. However, for some protein monolayers [13,25] and very cohesive lipids [26,27], the slope of the isotherm depends on the position of the sensor (a rectangular Wilhelmy plate) since the usual compression mode is asymmetric [28] (see Fig. 2.1), and thus the mechanical perturbation made in the film is both a compression–expansion and a shape perturbation. In the case of highly cohesive films, the response under the asymmetric perturbation will be affected by both the shear (G^*) and the compressibility (E^*) moduli, according to the following equations [28]:

$$|E^* + G^*| = A_0 \frac{\partial \pi_{\parallel}}{\partial A} \tag{2.1}$$

$$|E^* - G^*| = A_0 \frac{\partial \pi_{\perp}}{\partial A} \tag{2.2}$$

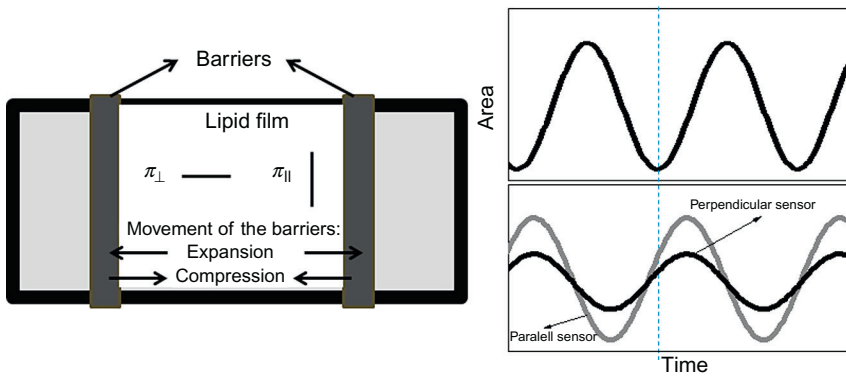

Figure 2.1 Left: Scheme of a typical experiment with two moving barriers. The two positions of the sensor relative to the movement of the barriers are represented. Right: The area of the film is perturbed sinusoidally, and the response is determined with the sensor at the different positions. In this example, the response shows a nonzero shear behavior, since the amplitudes detected with the sensor at different positions are different. The film is viscoelastic and not purely elastic, since the maximum compression (minimum area) is not synchronized with the maximum surface pressure (see vertical line).

where $\pi_{\parallel}$ and $\pi_{\perp}$ refer to the surface pressure determined with the sensor positioned parallel or perpendicular to the barriers, respectively (see Fig. 2.1). In turn, G^* and E^* can be expressed as:

$$G^*(\omega) = G'(\omega) + iG''(\omega) = G'(\omega) + i\omega\eta_s(\omega) \tag{2.3}$$

$$E^*(\omega) = E'(\omega) + iE''(\omega) = E'(\omega) + i\omega\eta_d(\omega) \tag{2.4}$$

Both parameters ($G^*$and E^*) are complex numbers with a real (elastic response) and an imaginary (viscous response) part, as is clear in Eqs. (2.3) and (2.4). The imaginary parts arise from the fact that the compression speed is finite, so there may be friction resisting the compression flow, and the resistance is characterized by the compression (dilatational) viscosity, η_d. On the other hand, the shear elastic viscosity, η_s, is the ratio between the shear stress and the rate of shear. In order to obtain each component of $G^*$and E^*, a sinusoidal perturbation in the film area may be performed with a frequency ω [25]. An instantaneous response is characteristic of an elastic material, whereas a retarded response indicates viscoelasticity.

For most lipids, however, shear can be neglected and the elastic compressibility can be directly obtained by the elastic compressibility modulus $\varepsilon = -\mathrm{MMA}(\partial\pi/\partial\mathrm{MMA})$. For lipid molecules with high intermolecular cohesion, strong lipid–lipid attractions are present within molecules that form the monolayer, and the resulting film has a high ε value, in the order of 10^2 mN/m (these are named "liquid-condensed") or higher (named "solid") [18]. In contrast, when lipids with low intermolecular interactions are spread at the air–water interface, softer films are formed (compressibility modulus from 10^1 to 10^2 mN/m), named "liquid-expanded" monolayers [18]. For intermediate interactions, phase transitions induced by compression can be observed. The phase state can also be modulated by temperature like any 3D-phase state: an increase in temperature decreases the surface pressure of the phase transition from an expanded to a denser phase state.

The phase transitions in pure lipid monolayers are first order, since two phases can be detected in the monolayer using different techniques. According to the Gibbs phase rule when applied to 2D systems by Crisp [1], lateral pressure should remain constant during the whole transition of monolayers composed of a pure lipid, and therefore, the compressibility modulus should be zero at equilibrium. However, during the phase transition of pure lipids, the isotherm generally shows a nonzero but low slope (see, e.g., Fig. 2.2A, gray line). Observation of this region of the isotherm

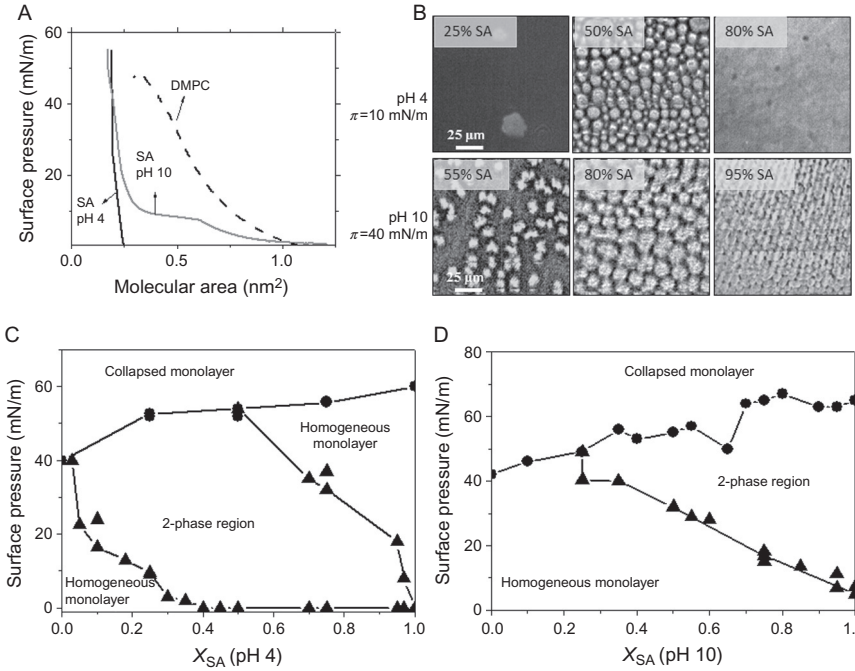

Figure 2.2 (A) Compression isotherms for DMPC and SA on subphases at pH 4 and 10. (B) Representative images for monolayers composed of SA and DMPC taken with BAM at the indicated pH, surface pressure, and lipid proportions. In this technique, condensed domains appear brighter. (C) Phase diagram for SA and DMPC on subphases at pH 4. (D) Phase diagram for SA and DMPC on subphases at pH 10. *Adapted from Caruso* et al. *[29] with permission.*

(normally called "plateau") has been reported frequently and studied from different points of view. The simplest explanation given for the lack of constancy of surface pressure during the phase transition is related to the presence of impurities [30,31], other explanations consider undulation of the in-plane concentration of surfactants [32], the presence of clusters [33–35], kinetic effects [36], and electrostatic repulsions [37]. Nevertheless, it is still an unresolved issue.

Monolayers can be observed while compressed by two techniques: fluorescence microscopy (FM) or Brewster angle microscopy (BAM). Both techniques detect the presence of two phases at the micron scale. Thus, the composition and lateral pressures at which they appear or disappear can be determined and plotted in a phase diagram (see, e.g., Fig. 2.2C and D).

In FM, a fluorescent lipid at a low proportion (1 mol% or lower) is added to the lipid solution before spreading. Lipids with a fluorescent moiety in the polar head group are bulky, and thus, in two-phase monolayers, their concentration is higher in the less dense phase. Consequently, this phase will be brighter than the denser phase, allowing observation with a microscope [6]. Images can be acquired using a fast CCD camera (10–50 frames/s), making it possible to record time series of the film. The movie can then be analyzed, and the dynamics of the film can be studied (see Section 5).

The other technique, BAM, can be utilized to image Langmuir monolayers with the advantage that no probe has to be added. A p-polarized laser beam is impinged on a clean air–water interface at the Brewster angle, that is, the angle at which reflected light is minimal. If a surfactant film is then formed at the interface, the properties of the reflected light will depend on the thickness and refractive index of the lipid monolayer [38]. Film thickness (h) can be calculated from the BAM images taken after the BAM equipment has been calibrated, provided that the refractive index of the film is known. For this, the gray level of each section of the micrograph is converted to reflected light intensity (R_p), and h is calculated assuming a smooth but thin interface in which the refractive index varies along the normal of the interface on a distance h, much smaller than the incident light wavelength Λ [38], which leads to:

$$h = \frac{\sqrt{R_p}}{\sin(2\theta_B - 90)} \left(\frac{\pi \sqrt{n_1^2 + n_2^2}\left(n_1^2 - n^2\right)\left(n_2^2 - n^2\right)}{\Lambda(n_1^2 - n_2^2)n^2} \right)^{-1} \tag{2.5}$$

In Eq. (2.5), n, n_1, and n_2 are the film, air, and subphase refractive indexes, respectively, and θ_B is the Brewster angle. The refractive indexes commonly used are in the range 1.42–1.50 for films in a condensed phase state [39,40], 1.36–1.44 for monolayers in an expanded phase state [40,41], and 1.00 for air. The subphase refractive index is usually close to that of water (1.33) and can be determined for each experiment from the experimental Brewster angle. When two phases are present, the condensed phase is thicker and presents a higher refractive index, thus reflecting more light and appearing brighter in the images (see examples in Fig. 2.2B).

Another important property of lipid membranes that can be determined using Langmuir monolayers is the electrical potential profile across the interface between the bulk aqueous phase and the hydrocarbon region. This potential arises from the fact that surfactants are dipolar molecules oriented normal to the plane of the interface [1,42–44]. In addition, the polar head

group is highly hydrated with a variable number of water molecules (depending on the polar moiety and the phase state) strongly bonded to the amphiphile [3]. These water molecules and also ions that interact strongly with the polar head group may also be responsible for the measured potential [32]. Besides, an electrical double layer of ions is formed in the case of films prepared with ionizable surfactants [1].

The surface potential can be determined in monolayers using two electrodes: a reference electrode in the subphase and a second electrode in the air, close to the monolayer. Two methods are used for the measurement of the potential, depending on the characteristics of the second electrode: the vibrating plate (Kelvin) method and the ionizing electrode method. Both techniques have been detailed elsewhere [1,42], and the potential values normally found for lipid monolayers using either of these methods are in the range of 100–500 mV (positive in the hydrocarbon chains region). This is the potential value normal to the plane of the monolayer, and it results from the combination of all the previously mentioned factors: bond dipoles in the hydrocarbon chains and in the polar head groups, and hydration water and ions in the subphase tightly interacting with the molecule. Although very elegant experiments have been performed in order to determine which of these factors contribute most [3,42,45–47], there is still no clear and accepted answer to this question. In any case, monolayers formed by different molecules have to be considered as different cases, and most probably all terms appreciably contribute to the final potential value.

Langmuir films have also been widely used to study the interaction and penetration of soluble molecules (anesthetics [48], proteins and peptides [49–56], vitamins [57], etc.) in membranes. These experiments were described in several reviews and will not be detailed here [1,54,56,58,59].

3. PHASE DIAGRAMS: TWO-PHASE REGIONS

As already mentioned, during phase transition of pure lipid monolayers, two phases coexist. Mixed monolayers can also be prepared and characterized, and when they are composed of a lipid that forms liquid-expanded monolayers with another lipid that forms denser monolayers, it is usually found that the components mix only at low proportions (dilute solutions), while at intermediate concentrations, two bidimensional phases coexist. For example, Fig. 2.2A shows the compression isotherms of dimyristoylphosphatidylcholine (DMPC) and stearic acid (SA) at low pH (neutral form of SA) and high pH (ionized form of SA). The corresponding

phase diagrams at each pH are shown in Fig. 2.2C and D. Representative images obtained by BAM are presented in Fig. 2.2B.

Alterations of the ionized state induce changes in the lipid–lipid interactions, leading to more expanded monolayers as the SA dissociates. A transition from a liquid-expanded to a liquid-condensed phase can be observed at pH of 10 (see plateau in Fig. 2.2A [40]). The miscibility of DMPC with SA in a liquid-expanded phase is high, and the phases segregate only when the SA monolayer reaches a condensed phase. Therefore, a change in the subphase pH leads to a change in the phase diagram, as may be noted when comparing Fig. 2.2C with D. Figure 2.3A shows this effect in a more noticeable manner: the molar fraction of SA at which

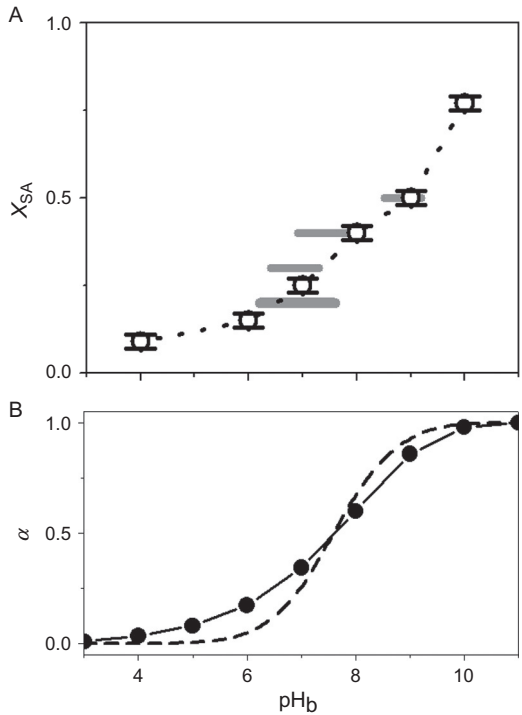

Figure 2.3 (A) Mole fraction of stearic acid at which phase segregation occurs at 17 mN/m, 20 °C and an ionic strength of 30 mM as a function of the subphase pH. Gray lines: the phase transition is driven by pH changes at constant surface pressure. Symbols: the phase transition is driven by compression at constant pH. (B) Symbols: degree of ionization for a molecule organized in a surface calculated using the Gouy–Chapman model with a bulk pK_a of 4.9, a mean molecular area of 0.25 nm^2 and a subphase with an ionic strength of 30 mM at 20 °C. Dotted lines: calculated degree of ionization for a soluble molecule with a pK_a of 7.6. *Adapted from Vega Mercado* et al. *[40] with permission.*

two phases appear at a constant surface pressure (17 mN/m) is plotted as a function of the subphase pH. The data for Fig. 2.3A were obtained by compressing the monolayer at constant pH (circles) or by changing the subphase pH at a constant pressure (gray lines), showing that these experiments are exploring quasi-equilibrium states [40].

The change in the solubility of SA in a DMPC matrix is smooth, with the midpoint of this curve ($X_{SA} = 0.35$) corresponding to a subphase pH of 7.6 and not to a pH equal to the pK_a of the molecule in bulk (p$K_a = 4.9$). In general, this may be because the surfactant acid constant at the interface is different from the bulk value and/or because the anionic monolayer attracts cations, thereby generating a double layer of ions, and consequently, the surface pH is lower than the bulk pH of the subphase. Assuming that the acid constant of the surfactant forming a supramolecular structure is similar to that of the surfactant in bulk (which was reported to be the case for fatty acids [1]) and that the surface pH (pH_s) differs from the bulk pH (pH_b) according to a Boltzmann distribution, the surface pH will vary according to the following equation:

$$pH_s = pH_b + \frac{F\Psi_0}{2.3RT} \tag{2.6}$$

where Ψ_0 is the double layer potential at the surface, F is the Faraday constant, and RT is the thermal energy. The double layer potential depends on the ionic strength of the subphase and on the ionization degree of the surfactant. According to the Poisson–Boltzmann equation, the surface charge density (σ) is related to the double layer potential and to the ion concentration in the bulk (C_i^{∞}) as [60]:

$$\sigma = \sqrt{2RT\varepsilon_0\varepsilon}\left[\sum_i C_i^{\infty}\exp\left(-\frac{Fz_i\Psi_0}{RT}\right) - \sum_i C_i^{\infty}\right]^{1/2} \tag{2.7}$$

The sum is taken over all the ionic species i present in the subphase, ε_0 is the permittivity in vacuum, ε is the relative permittivity of the medium, and z_i is the valence of the i ion.

On the other hand, the surface charge generated by a monolayer with an average molar area A, formed by an ionizable surfactant with acid constant K_a^s, according to which the species distribution (α) depends on the surface proton concentration $[H^+]_s$, is given by:

$$\sigma = -\frac{F\alpha}{A} = -\frac{F}{A}\left(\frac{K_a^s}{K_a^s + [H^+]_s}\right) \tag{2.8}$$

Thus, equating Eqs. (2.7) and (2.8) and resolving numerically the resulting equation leads to the solution of the system. The symbols in Fig. 2.3B show the fraction of ionized molecules, α, calculated using this approach (for details see Vega Mercado *et al.* [40]), and the trend followed by α is similar to that of the solubility of SA in the DMPC monolayer. Furthermore, the value of the bulk pH at which $\alpha = 0.5$ corresponds to 7.6. This is termed the "apparent pK_a," or in other words, the value of the bulk pH at which the interface senses a $pH = pK_a = 4.9$. It is worth remarking that the ionization of molecules organized at interfaces shows a low cooperative α profile (from $pH \sim 4$ to $pH \sim 10$ in this example, i.e., ± 3 pH units from the apparent pK_a value). Moreover, the pH range where α changes is broader than the expected profile for a molecule in bulk, which is considered to be completely dissociated/associated at $-2/+2$ pH units from the pK_a value. For comparison, the dissociation profile for a molecule in bulk with $pK_a = 7.6$ is plotted in Fig. 2.2B (dashed lines), highlighting the broadening of the dissociation profile of a molecule organized at a surface. This effect appears as a consequence of the generation of the double layer, which changes the surface pH as the molecule ionizes. In other words, as the bulk pH increases beyond the surfactant pK_a, the surface pH does not change in the same fashion, since the electrical double layer acts as a buffer, resulting in a more acid interface and a less charged monolayer than that expected in the absence of the cloud of contraions. Hence, this effect is less marked when the ionic strength of the subphase is high, since the surface charge is screened at closer distances and by other ions that are different from H^+ [57,61], thus suggesting that salt concentration is another parameter regulating the mixing–demixing regions of the phase diagrams of mixtures with an ionizing component.

It is worth mentioning here that, in the approach presented, the monolayer was considered an array of charges in a plane with a density equal to the molecular density. However, the charged interface corresponds to charged polar head groups that may interact specifically with certain ions [62] and that are subject to thermal fluctuations (and thus the density and out-of-plane positions fluctuate). Nevertheless, this approach makes it possible to estimate the effects of a charged monolayer on the local pH value. Related to this, the distribution of ions close to a charged membrane obtained with molecular dynamics simulations was compared to the trend predicted by the

Gouy–Chapman model (with the same assumptions as the approach detailed here) and a good match was found [63].

4. DISTRIBUTION OF THE PHASES IN THE PLANE OF THE MONOLAYER

In the region of phase coexistence, surfactant monolayers show inhomogeneity in molecular density. At low proportions of the molecule that forms the more rigid monolayers, clusters of surfactants in a denser phase state are surrounded by surfactants in a more expanded phase state with these clusters being termed "domains" (or "rafts" for some particular lipid compositions [64]). As the amount of the surfactant in the denser phase state increases (as a consequence of changes in surface pressure, temperature, film composition, etc.), the domains increase in size and/or number until they come into contact with each other. At this point (the percolating point), the denser phase becomes the continuous phase.

Two-component lipid phase separation can be thought of as a 2D fluid in which one component is crystallizing from the less dense phase. According to the classical theory of nucleation, the line tension (λ) between a crystallizing phase and the surrounding medium controls the rate of nucleation [65]. The line tension may be defined as the change of free energy upon an infinitesimal elongation of the phase boundary. In the absence of long-range electrostatic interactions, this free energy change does not depend on how the elongation is brought about. Hence, λ is a quantity entirely defined by equilibrium properties. However, when electrostatic interactions become important, the free energy increase becomes dependent on the deformation mode and is thus no longer an equilibrium property [66].

The classical theory of nucleation predicts that the rate of nucleation decreases exponentially with λ and the size of a critical or stable nucleus increases linearly with λ. Thus, line tension will influence the number of nuclei (nuclei density) and, therefore, the distance between neighboring nuclei. Once nucleation has occurred, the nuclei grow to micron-sized domains, and it has been reported that the size (and also the overall shape, see below) of the domains depend on the position of the nucleation points relative to the surrounding nucleation point positions [67,68], that is, the spatial distribution of the nucleation points, markedly influenced by the line tension, regulates the domain size. As an example of the effect of nuclei density on domain size, Fig. 2.4 shows the texture of a monolayer in which the nuclei density has been modified by the application of an inhomogeneous

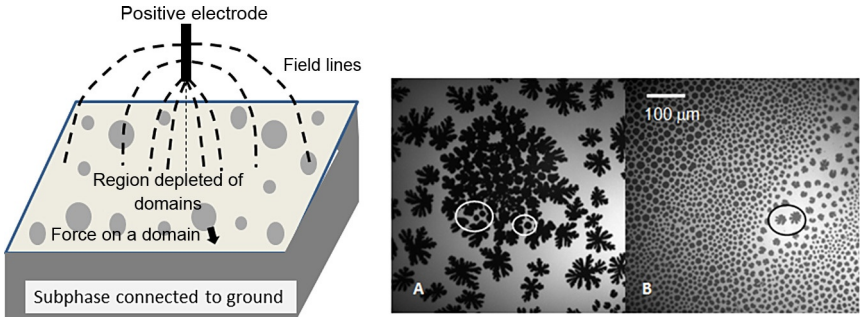

Figure 2.4 Left: scheme of the experimental setup for the application of an inhomogeneous electrostatic field to a Langmuir monolayer. Right: monolayer composed of SA and DMPC in a proportion of 40 (A) or 55 (B) mol% of SA on subphases at pH 4. In panel (A), the domains in a film at 1 mN/m were regionally attracted for 2 min using an inhomogeneous electric field (300 V). The field was switched off, and the film was compressed to 17 mN/m. A field of the same intensity but opposite polarity was applied in (B) at low lateral pressures, and afterward, the monolayer was further compressed. The micrograph was taken using FM, and thus domains appear darker. *Adapted from Vega Mercado* et al. *[68] with permission.*

electrostatic field (see scheme in Fig. 2.4). This field induces the migration of the domains from or to the region under the electrode, depending on the sign of the applied potential and the dipole moment density of the domain relative to the continuous phase [47,69–71]. Once a region has been crowded (Fig. 2.4B) or depleted (Fig. 2.4C) of domains, the field is turned off and the domains are grown by further compressing the monolayer. The heterogeneous distribution of domains remains stable for minutes (sometimes hours), thus allowing domain growth to be studied in different environments. Figure 2.4 shows that domains that have grown in a crowded region are smaller than domains that grew in regions with lower domain density: in Fig. 2.4A, the encircled domains are small and the rest are large, while in Fig. 2.4B, domains are small in the whole monolayer except in the region depleted of domain (encircled region) [68].

Line tension is a consequence of the different lateral interactions experienced by the molecules placed in the domain border relative to those that are far from the edge. Commonly, the thickness of each phase (h) is different, and thus, if the orientation and length of the lipids were the same as they are at some distance from the boundary, an abrupt change in thickness would exist at the domain boundary, that is, a hydrophobic mismatch δ. However, lipids very probably deform at the boundary so as to prevent the creation of an abrupt thickness change. The possible lipid deformations are three: splay

(a generalization of bending), tilt, and area compression; line tension is proposed to depend on all these factors. A theoretical model developed by Cohen's group [72–74] derived the following equation for the line tension in lipid bilayers:

$$\lambda = \frac{\sqrt{B_1 K_1 B_2 K_2}\,\delta^2}{\sqrt{B_1 K_1} + \sqrt{B_2 K_2}\,h^2} - \frac{(J_1 B_1 - J_2 B_2)^2}{2\sqrt{B_1 K_1} + \sqrt{B_2 K_2}} \tag{2.9}$$

where B_1 and B_2 are the splay elastic moduli, K_1 and K_2 are the tilt moduli, and J_1 and J_2 are the spontaneous curvatures of phases 1 and 2, respectively. The model considers symmetric membranes and not lipid monolayers, and it has been used successfully in order to calculate λ in both, monolayers and bilayers [75,76], with the inconvenience that not all the moduli may be known and some values are usually assumed.

An approximate equation for λ at the domain boundary in lipid monolayers has also been derived in terms of the hydrophobic mismatch δ [77]. Similar to bilayers, the derived equation indicates that λ depends on δ and on the energy needed to deform the lipids in the boundary region. The equation derived by Lee *et al.*, however, relates λ with the experimental deformation geometry of the monolayer and not with the intrinsic deformability moduli of the lipid membrane, and therefore, a direct comparison with Eq. (2.9) cannot be performed.

Line tension has also been determined experimentally using various approaches (for a recent review, see Sriram *et al.* [78]). In the case of deformable domains, the relaxation of the shape of a previously deformed domain is studied, and from this process, λ is obtained. Domain deformation has been performed in different ways, starting from the pioneering experiments of McConnell's group, in which a flux is applied to the subphase thereby promoting a drift on the monolayer [79–81]. Domains have also been deformed by the use of optical tweezers [82] and electric fields [83]. For systems close to a critical point, the fluctuation of the domain shape has been analyzed in order to determine λ in monolayers and also in bilayers [84–86]. In the case of bilayers, micropipette aspiration has also been applied [87].

For nondeformable domains, these methods cannot be applied. Longo's group determined the line tension of stiff domains using the nucleation rate of the domains [65,88,89]. The size distribution of domains would also provide information of the value of the line tension if at equilibrium, and it has been used with this purpose [77,90]. However, equilibrium size distribution is not reached easily [68,91].

In summary, line tension is an important factor for a phase nucleation and the subsequent growth of the nucleus to form a microscopic domain. Therefore, efforts have been made to describe the factors underlying the line tension in monolayers and in bilayers, but a good understanding of the factors regulating this parameter is still lacking. Knowing how to manipulate line tension would permit modulation of the texture of a biphasic monolayer, which has been performed by introducing in the monolayer a molecule that partitions preferentially in the domain boundary (a "lineactant") [78,92–95].

Regarding domain shape, different monolayer systems with phase coexistence have been studied and a variety of textures have been reported. Lipid domains exhibit intriguing microscopic shapes, with both the lipid head group and the hydrocarbon chain moiety being important determinants of domain morphology [96,97]. Nonrounded shapes in equilibrium forming ordered patterns in the plane of the monolayer suggest the presence of intermolecule long-range repulsions [66], which have been assigned to the dipolar repulsions that arise from the fact that surfactants are dipolar molecules oriented normal to the plane of the interface. As mentioned earlier, water and ions that interact strongly with the polar head group may also be responsible for the dipolar potential as well as for the intermolecular repulsions [32].

McConnell proposed the "equivalent dipole model" to evaluate the effect of electrostatics in biphasic lipid monolayers at the air–water interface. In this model, the lipid molecules as well as all ions and water molecules are replaced by a hypothetical two-dimensional planar array of dipoles, with the number density of these dipoles being assumed to be of the same order of magnitude as the number density of the molecules at the air–water interface. For systems with cholesterol, where two isotropic bidimensional liquids coexist, the equivalent dipoles are all oriented perpendicular to the monolayer plane [98], since other components can be neglected due to the averaging caused by precession motion. This model predicts that the equilibrium shape of the domains is determined by three major forces: line tension at the domain boundary, dipolar repulsion inside the domains, and domain–domain dipolar interactions [15], with the balance between line tension and dipolar repulsions determining the critical size for a shape transition from rounded to branched domains. The validity of this model has been tested on a broad variety of systems, and a good match has been found between theory and experimental results [75,96,99–108].

Although many studies focusing on the shape of neutral domains have been performed, there are few studies related to charged domains. Janmey's group formulated a mathematical approach similar to the one presented by

McConnell's group, but by considering a net charge on each molecule forming the domain. Compared to a neutral domain, the free energy of the domain has an additional term that takes into account the effect of charge–charge repulsion on the domain shape. Then, as expected, they found that at a high charge density, a noncircular shape minimizes the domain energy and the critical size at which instability occurs, increases with the ionic strength [109,110]. In addition, Loverde *et al.* [111] explored the asphericity of charged domains using molecular dynamic simulations and also found that increasing the electrostatic contribution influences the shape of the domains and strongly increases correlation and ordering between domains.

In the case of rigid domains, the domain shape has been related to the closer lipid–lipid interactions, in analogy to 3D crystals. Thus, preferential regions of domain growth have been linked to the chirality of the molecule, since chiral interactions emerge when the molecules are packed closely [104,112,113].

On the other hand, different to the cases discussed of equilibrium domain shapes, fast growth leads to out-of-equilibrium shapes, where morphological instability and irregular growth have been described [65,68,96,114,115]. For unequilibrated oversaturated systems, the competition between the rates of phase segregation and molecular migration to the domain (mainly through Marangoni flow [114,115]) determines whether the growth is reaction limited or migration limited. Slow phase segregation (low oversaturation) leads to reaction-limited growth and domains with equilibrium shapes, whereas high oversaturation leads to migration-limited growth and fractal domains with branched morphologies, [88,103] which relax to more rounded shapes [68].

5. IN-PLANE INTERACTIONS AND CONSEQUENCES ON FILM EFFECTIVE RHEOLOGY

The presence of domains formed by lipids in a dense phase state affects the mechanical properties of the monolayer, since the domains act as rigid obstacles. The elastic compressibility of a two-phase monolayer at a constant surface pressure increases as the percentage of area occupied by the phase forming the domains (%AC) increases. In Fig. 2.5A, a normalized compressibility is plotted as a function of the %AC for eight different mixtures in which the phase that forms the domain is stiffer than the other phase [29]. An abrupt change in the compressibility modulus is observed at a value of %

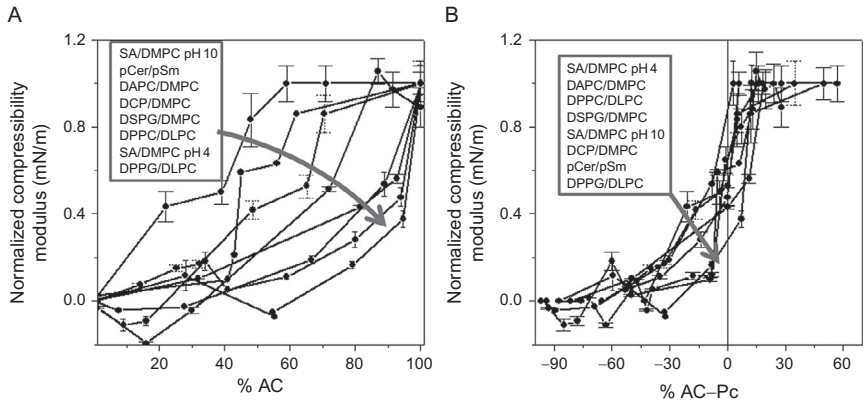

Figure 2.5 (A) Normalized compressibility modulus as a function of the percentage of condensed area (%AC). The lipid mixtures are stearic acid with dimyristoylphosphatidylcholine at pH 4 and 10 mN/m (SA/DMPC, pH 4), dihexadecyl phosphate with dimyristoylphosphatidylcholine at 10 mN/m (DHP/DMPC), dipalmitoyl phosphatidylglycerol with dilauroyl phosphatidylcholine at 10 mN/m (DPPG/DLPC), distearoyl phosphatidylglycerol with dimyristoylphosphatidylcholine at 20 mN/m (DSPG/DMPC), diarachidoyl phosphatidylcholine with dimyristoylphosphatidylcholine at 20 mN/m (DAPC/DMPC), dipalmitoyl phosphatidylcholine with dilauroyl phosphatidylcholine at 30 mN/m (DPPC/DLPC), stearic acid with dimyristoylphosphatidylcholine at pH 10 and 40 mN/m (SA/DMPC, pH 10), and palmitoyl ceramide with palmitoyl sphingomyelin at 5 mN/m (pCer/pSm). (B) Same parameter as a function of %AC minus its percolation threshold (Pc). *Adapted from Caruso* et al. *[29] with permission.*

AC that depends on the mixture and coincides in all cases with the value of % AC, where the stiffer phase percolates, as shown in Fig. 2.5B where the normalized compressibility modulus is plotted against the percentage of condensed area minus the corresponding value at percolation (Pc). In other words, for a two-phase monolayer with one phase stiffer than the other, the presence of condensed domains slightly increases the stiffness of the monolayer until the percolating phase becomes the condensed phase, where the rigidity of the monolayer becomes similar to that of the condensed phase, regardless of the presence of the expanded phase in corrals formed by the condensed phase.

Regarding the film response under shear stress, the presence of domains strongly affects the diffusion of the other species present in the monolayer, reaching a null long-time diffusion coefficient as the denser phase area fraction approaches the percolation threshold [116,117]. Domains provide an inhomogeneous scenario with regard to not only their rheological properties but also their electrostatics. The electrostatic field generated by the domains

can attract or repel the diffusing components, thus influencing their lateral motion [118,119].

The diffusion coefficient (D_{exp}) of micron-sized domains inserted in a liquid-expanded phase can be determined by tracking the position of a domain relative to other domains of similar size and bearing similar drift in the monolayer, since the slope of the plots of the relative mean square displacement (MSD_{rel}) as a function of the lapse time (Δt) is equal to $8D_{exp}$ [24,120–122]. It has been observed that the value of the diffusion coefficient determined in this way depends on the distance between the domains in the monolayer as shown in Fig. 2.6A, where the diffusion coefficient of small domains (5–10 μm^2) is plotted as a function of the interdomain distance for monolayers composed of ceramide and sphingomyelin at two different lateral pressures [121]. In this experiment, domains are isolated by the application of an inhomogeneous repulsive electric field (see scheme in Fig. 2.4), which is turned off once the desired array of domains is achieved, and then domains in this new environment are tracked. The increase in the diffusion coefficient as domain density decreases is clearly not caused by a change in the intrinsic viscosity of the continuous phase but is due to the interdomain repulsions that preclude movement of the analyzed pair of domains. From

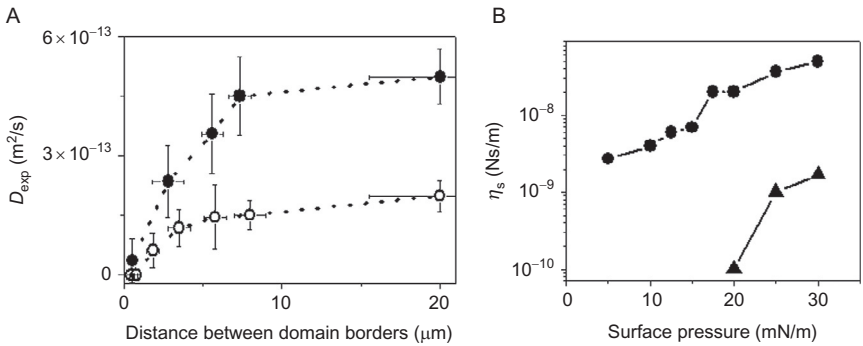

Figure 2.6 (A) Domain diffusion coefficients for small domains (5–10 μm^2) as a function of the distance between neighboring domain–domain borders on 0.15 M NaCl solutions at 5 (black symbols) and 25 (open symbols) mN/m. Monolayers are composed of 10 mol % of palmitoyl ceramide and 90 mol% of palmitoyl sphingomyelin. (B) Membrane apparent viscosity as detected from the movement of small domains (5–10 μm^2) as a function of the lateral pressure on 0.15 M NaCl (black symbols). The circles correspond to data obtained from isolated domains (domain–domain distances higher than 10 μm) and the triangles to domains in the normal array (domain–domain distances between 1 and 3 μm depending on the surface pressure). The monolayer composition is the same as in panel (A). *Adapted from Wilke* et al. *[121] with permission.*

the diffusion coefficient obtained, an apparent monolayer viscosity can be estimated, that is, the viscosity sensed by the domain in its environment. This is performed following the equations derived by Hughes *et al.* [123], which relate the motion of a cylinder in a membrane with the membrane surface viscosity η_S [121,122]. Figure 2.6B shows the surface viscosity calculated following this approach for isolated domains (triangles) and for domains in the array normally found for the palmitoyl ceramide/palmitoyl sphingomyelin mixture in these conditions (circles). Domains are named "isolated" at domain densities low enough, so that the diffusion coefficient no longer changes, that is, at a distance of about 10 μm in this example (see Fig. 2.6A). Therefore, the triangles correspond to the intrinsic viscosity of the monolayer while the circles represent increased viscosity due to interdomain repulsions.

The intrinsic viscosity may be calculated following this approach in this system at surface pressures of 20 mN/m or higher, that is, for surface pressures where palmitoyl sphingomyelin (the lipid that forms the continuous phase) is in a condensed state [121]. However, the surface viscosity of liquid-expanded monolayers is usually in the order of 10^{-10} Ns/m [24,121], and for this value, the motion of micron-sized domains is expected to depend only on the subphase viscosity (η_w) and their size, according to $D_t = k_B T/8\eta_w R$ [123], where k_B is the Boltzman constant, T is the temperature, and R is the radius of the analyzed domain. Thus, the value of the diffusion coefficient determined experimentally (D_{exp}) should equal the value of the diffusion coefficient (D_t) calculated for noninteracting particles in a liquid-expanded environment. Differences found in the values of D_{exp} compared to D_t are assigned to the presence of hydrodynamic and electrostatic repulsions (the latter being preponderant [122]) between the moving species, which precludes their movement and, therefore, translates to a lower value of D_{exp} [24,121,122]. Therefore, the diffusion coefficients of domains and particles have been used to estimate the strength of the interactions between domains and the moving species [24,118,119,121,124,125].

Using this approach, the influence of the ionic strength of the subphase on interdomain interactions was studied for charged domains of dipalmitoyl phosphatidylglycerol, and it was found that these interactions can be modulated with the salt concentration in the subphase, as emerged when comparing the black symbols with the gray symbols in Fig. 2.7A and B. At high ionic strength, charged domains repel similarly to neutral domains (open symbols), while at low ionic strength solutions, domain motion is highly precluded. This observation was interesting since, in the low ionic strength

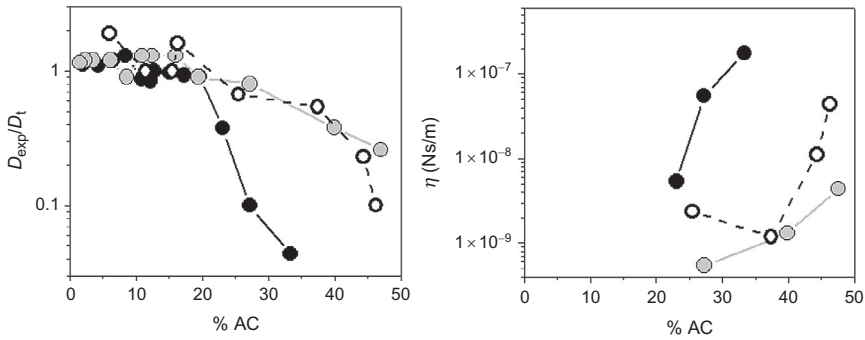

Figure 2.7 (A) Diffusion coefficients normalized by the diffusion coefficient for a monolayer with negligible viscosity and interdomain interactions as a function of the percentage of area occupied by the domains (percentage of condensed area, %AC). (B) Apparent surface viscosity as a function of %AC calculated from the diffusion coefficient of domains following the model of Hughes *et al.* [123]. Symbols: dipalmitoyl phosphatidylglycerol monolayers in the presence (gray) and absence (black) of 0.15 M NaCl in a TRIS buffer subphase at 21 °C and neutral phospholipids (DSPC/DMPC) on 0.15 M NaCl (open symbols) at 23 °C. *From Caruso* et al. *[122] with permission.*

solutions, the Debye–Hückel length was still two orders of magnitude lower than the interdomain distances, and thus the charge of the domains would be screened also in these salt conditions. Nevertheless, the interdomain interactions were able to reflect the decrease in the charge screening, indicating that domain–domain electrostatic interactions are able to regulate the film's rheological properties even at conditions where interdomain distances are higher than the Debye–Hückel distance. This is probably a consequence of the fact that electrostatic interactions may occur not only through the aqueous subphase but also within the plane of the monolayer where the ionic double layer is absent.

The apparent surface shear viscosity was also computed with a magnetic needle [126], and the authors found that its variation with the percentage of condensed area was analogous to that of a three-dimensional dispersion of spheres in solvent with long-range repulsive interactions [126].

Regarding diffusion species different from a domain, Nassoy *et al.* [119] showed that a partially ionized latex particle inserted into a surfactant monolayer is attracted to the border of domains composed of neutral molecules in a liquid-condensed phase, due to the dipolar interactions. These authors determined an electric field of −30 V/cm at the domain border, which generated an attractive potential on the bead as high as 300 $k_B T$. Related to this, Forstner *et al.* [118] modeled systems far from the percolation threshold and found a dramatic slowing down of diffusive propagation, not caused by

geometric effects but by the presence of electrostatic interactions between a dipolar domain and a dipolar diffusing species. When numerical simulations were used for a systematic study of these diffusion processes in monolayers, a sensitive dependence on the interaction strength was found: small differences in the potential result in orders of magnitude changes of the long-term diffusion coefficient. In addition, the interaction strength can be easily altered by changing the domain size, regardless of domain composition [118]. The same research group also found that there is an electrostatic potential strength threshold, marking a sharp transition from almost unaltered free diffusion to a diffusive process with a drastically reduced diffusion coefficient. In other words, two diffusing species with only a small difference in their interactions with domains will have significantly different propagations within the same environment. Thus, the presence of domains can selectively regulate the diffusion of a particle, according to the electrostatic properties of the particle and the size of the domain [118].

Not only the domain size but also its shape influences the diffusion of a dipolar species close to a domain, since branched domains generate intense electric field zones in the more curved regions of the domain periphery [127]. Thus, a small circular domain influences the motion of particles inserted in the monolayer in a different manner to larger flower-like domains. As already discussed, this effect can be amplified in a monolayer with different effective mechanical properties due to local electrostatics, deriving in other possible consequences. For example, the activity of membrane-active lipolytic enzyme reactions was shown to regulate the texture of the membrane, and in turn, the texture regulates the velocity of the catalyzed reaction [22,127].

6. COMPARISON BETWEEN DIFFERENT MODEL MEMBRANES

Different model membrane systems have been used successfully in order to gain insight into cell membrane properties. In spite of the fact that none of them reflects the enormous complexity of real membranes, they help to understand local properties derived from the interactions between a few molecules.

The use of different model membranes permits a wide variety of experimental approaches: in Langmuir monolayers, molecular density can be varied while surface tension and surface potential are registered, and the membrane can be simultaneously observed with BAM or FM. Using FM, giant unilamellar vesicles (GUVs) can also be investigated along with the

deformations out-of-plane of the membrane. In planar free-standing bilayers, particle tracking and membrane permeability may be determined in a simpler way than in GUVs, but the film stability is lower. The supported lipid bilayers are usually deposited on a hydrophilic solid surface (glass, mica, or silicon) using several preparation techniques such as spin coating [128], vesicle rupture [129], solution spreading [130], or film transfer from a Langmuir monolayer through the Langmuir–Blodgett or the Langmuir–Schaefer technique [131]. The main advantage of supported lipid bilayers over water/air interface monolayers or vesicular systems is that they may be characterized by using a number of advanced techniques, such as atomic force microscopy [131] and quartz crystal microbalance [132].

Each of these model systems has certain advantages and disadvantages, and it is worth asking which of them is more suitable to investigate membrane properties. Cell membranes in biological systems may not be similar to free-standing bilayers, since they are often interacting with (and supported by) cytoskeletal proteins, neighboring membrane stacks, and extracellular matrices, with these interactions affecting the native lipid phase behavior.

There are a few reports comparing the results for the same system forming different types of model membranes [133–143], and they indicate that the similarities and differences depend on the system analyzed and on which property is explored. The property of membranes that can probably be compared most easily between different models is the temperature for the phase transition. This temperature appears not to change [144] or to alter only slightly [134,139,145,146] in vesicles compared to that in supported membranes. In supported bilayers, however, two different transition temperatures for the distal (to the support) and the proximal leaflets have been reported [137,147].

The comparison of the properties of monolayers at the air–water interface with free-standing bilayers has to be performed at a defined surface pressure. It has been postulated that at between 30 and 35 mN/m, the MMA in bilayers is equivalent to that observed in monolayers [148,149], although thermal fluctuations may lead to variations in the lateral pressure [150]. Assuming a correspondence between bilayers and monolayers at 30–35 mN/m, a comparison of the phase transition for lipids forming 3D aggregates and for the same lipids forming monolayers has been performed, and it has been proposed that the transition temperature roughly coincides for phospholipids [151] and some glycosphingolipids [20,152]. However, as the glycosphingolipid polar head group becomes more complex, the differences in the relative sizes of the oligosaccharide chain and the hydrocarbon

moiety introduce curvature tensions in the self-assembled structure, affecting the overall topology, and the lateral phase state and the transition temperature for the 3D aggregates is lower than the temperature at which a fully liquid-expanded state is acquired in the flat two-dimensional monolayers [152,153].

Changes in temperature for the phase transition may translate to changes in the phase diagram, and thus the composition of the coexisting phases in mixed films may not be exactly the same at the different interfaces [143].

The phase diagrams of monolayers and GUVs composed of ternary mixtures with cholesterol have been compared by Keller's group, with the inconvenience that cholesterol oxidizes at the air–water interface, concomitantly changing the mixture properties [135]. These authors observed correlations between miscibility in bilayers and in monolayers of a saturated phosphatidylcholine lipid, an unsaturated phospholipid, and cholesterol [142]. Only limited overlap in miscibility phase behavior was found for monolayers and bilayers of mixtures composed of DOPC/DPPC/Chol and POPC/PSM/Chol [136]. Regarding membrane texture, it has been proposed that electrostatic interactions would be not so important in bilayers compared to monolayers, due to the charge screening by the aqueous solution [154], and curvature tensions appear to be important factors [155].

Other properties of the transferred film are not exactly the same as those of the Langmuir monolayer, with the differences depending on the characteristics of the support, the film, and the film-solid interactions [133,134]. Even without considering specific interactions between the solid support and the surfactant film, an entropy reduction due to the presence of the solid support may lead to slightly different phase diagrams when comparing free-standing with solid-supported films [138,143]. In addition, when comparing the same system using the same model membrane, differences have been found depending on the preparation methods. In supported films formed through the rupture of vesicles [156], it has been demonstrated that different experimental conditions lead to different film properties as regards the composition of each layer [157], the stabilities upon lipid flip-flop from the distal to the proximal leaflet or vice versa [129], reorganizations with a subsequent change in the film texture [135,136], and as surfactant diffusion [158].

7. SUMMARY

Langmuir monolayers composed of lipids permit the generation of highly controlled monomolecular thick films, which can be studied using

a broad variety of techniques and modifying the molecular density of the film. The results found using this system are comparable to those found in other model membranes, but may be quantitatively not equal, and a systematic evaluation of this is still lacking.

When two phases coexist, line tension at the domain borders appears to be an important factor for the determination of film texture, and thus, controlling this parameter would permit modulation of the domain shape and size, which is therefore an interesting area of research that has been little explored.

Valuable information regarding the effect of membrane texture on membrane rheology has been obtained from experiments using Langmuir monolayers. The elastic compressibility modulus is slightly affected by the presence of noncontacting domains formed by lipids in a dense phase state, while the apparent shear viscosity of the film (as sensed by a dipolar species) can be strongly increased due to the interactions between the domains and the moving species.

If the factors underlying the monolayer texture are known in a system, domain size and shape can be modulated, and consequently, the rheology and electrostatics of the interface are also in turn regulated.

ACKNOWLEDGMENTS

SECyT-UNC, CONICET, and FONCYT (Program BID 0770) helped with financial support. N. W. is a Career Investigator of CONICET. I am grateful to Dr. M.L. Fanani who read the chapter and provided critical comments.

REFERENCES

[1] G.L. Gaines, Insoluble Monolayers at Liquid-Gas Interfaces, Interscience Publishers, New York, 1966.
[2] H.L. Brockman, Lipid monolayers: why use half a membrane to characterize protein-membrane interactions? Curr. Opin. Struct. Biol. 9 (1999) 438–443.
[3] H.L. Brockman, Dipole potential of lipid membranes, Chem. Phys. Lipids 73 (1994) 57–79.
[4] R.E. Brown, H.L. Brockman, Using monomolecular films to characterize lipid lateral interactions, Methods Mol. Biol. 398 (2007) 41–58.
[5] G. Brezesinski, H. Mohwald, Langmuir monolayers to study interactions at model membrane surfaces, Adv. Colloid Interface Sci. 100–102 (2002) 563–584.
[6] H. Mohwald, Phospholipids monolayers, in: R. Lipowsky, E. Sackmann (Eds.), Structure and Dynamics of Membranes, Elsevier, Amsterdam, 1995, pp. 161–211.
[7] H. Mohwald, Phospholipid and phospholipid-protein monolayers at the air/water interface, Annu. Rev. Phys. Chem. 41 (1990) 441–476.
[8] N. Ahamad, D. Prezgot, A. Ianoul, Patterning silver nanocubes in monolayers using phase separated lipids as templates, J. Nanopart. Res. 14 (2012) 724–734.
[9] T. Mori, K. Sakakibara, H. Endo, M. Akada, K. Okamoto, A. Shundo, M.V. Lee, Q. Ji, T. Fujisawa, K. Oka, M. Matsumoto, H. Sakai, M. Abe, J.P. Hill, K. Ariga,

Langmuir nanoarchitectonics: one-touch fabrication of regularly sized nanodisks at the air-water interface, Langmuir 29 (2013) 7239–7248.
[10] M.J. Davies, T.D. Kerry, L. Seton, M.F. Murphy, P. Gibbons, J. Khoo, M. Naderi, The crystal engineering of salbutamol sulphate via simulated pulmonary surfactant monolayers, Int. J. Pharm. 446 (2013) 34–45.
[11] P.J. Sanstead, N. Florio, K. Giusto, C. Morris, S. Lee, Sensitivity of cationic surfactant templates to specific anions in liquid interface crystallization, J. Colloid Interface Sci. 376 (2012) 152–159.
[12] A. Tenboll, B. Darvish, W. Hou, A.S. Duwez, S.J. Dixon, H.A. Goldberg, B. Grohe, S. Mittler, Controlled deposition of highly oriented type I collagen mimicking in vivo collagen structures, Langmuir 26 (2010) 12165–12172.
[13] E.J. Grasso, R.G. Oliveira, M. Oksdath, S. Quiroga, B. Maggio, Controlled lateral packing of insulin monolayers influences neuron polarization in solid-supported cultures, Colloids Surf. B Biointerfaces 107 (2013) 59–67.
[14] Z. Xue, D. Hu, S. Dai, Z. Du, Crystallization and self-assembly of flowerlike superstructures of calcium carbonate regulated by pepsin Langmuir monolayers, Mater. Chem. Phys. 136 (2012) 771–777.
[15] H.M. McConnell, Structures and transitions in lipid monolayers at the air-water interface, Annu. Rev. Phys. Chem. 42 (1991) 171–195.
[16] D. Vollhardt, Supramolecular organisation in monolayers at the air/water interface, Mater. Sci. Eng. C 22 (2002) 121–127.
[17] A.W. Adamson, Physical Chemistry of Surfaces, Wiley, New York, 1982.
[18] J.T. Davies, E.K. Rideal, Interfacial Phenomena, Academic Press, NY, 1963.
[19] B. Maggio, I.D. Bianco, G.G. Montich, G.D. Fidelio, R.K. Yu, Regulation by gangliosides and sulfatides of phospholipase A2 activity against dipalmitoyl- and dilauroylphosphatidylcholine in small unilamellar bilayer vesicles and mixed monolayers, Biochim. Biophys. Acta 1190 (1994) 137–148.
[20] B. Maggio, M.L. Fanani, C.M. Rosetti, N. Wilke, Biophysics of sphingolipids II. Glycosphingolipids: an assortment of multiple structural information transducers at the membrane surface, Biochim. Biophys. Acta 1758 (2006) 1922–1944.
[21] B. Maggio, G.A. Borioli, B.M. Del, T.L. De, M.L. Fanani, R.G. Oliveira, C.M. Rosetti, N. Wilke, Composition-driven surface domain structuring mediated by sphingolipids and membrane-active proteins. Above the nano- but under the micro-scale: mesoscopic biochemical/structural cross-talk in biomembranes, Cell Biochem. Biophys. 50 (2008) 79–109.
[22] M.L. Fanani, S. Hartel, B. Maggio, T.L. De, J. Jara, F. Olmos, R.G. Oliveira, The action of sphingomyelinase in lipid monolayers as revealed by microscopic image analysis, Biochim. Biophys. Acta 1798 (2010) 1309–1323.
[23] C.M. Rosetti, B. Maggio, N. Wilke, Micron-scale phase segregation in lipid monolayers induced by myelin basic protein in the presence of a cholesterol analog, Biochim. Biophys. Acta 1798 (2010) 498–505.
[24] N. Wilke, F. Vega Mercado, B. Maggio, Rheological properties of a two phase lipid monolayer at the air/water Interface: effect of the composition of the mixture, Langmuir 26 (2010) 11050–11059.
[25] P. Cicuta, E.M. Terentjev, Viscoelasticity of a protein monolayer from anisotropic surface pressure measurements, Eur. Phys. J. E 16 (2005) 147–158.
[26] I. Lopez-Montero, E.R. Catapano, G. Espinosa, L.R. Arriaga, D. Langevin, F. Monroy, Shear and compression rheology of Langmuir monolayers of natural ceramides: solid character and plasticity, Langmuir 29 (2013) 6634–6644.
[27] E.R. Catapano, L.R. Arriaga, G. Espinosa, F. Monroy, D. Langevin, I. Lopez-Montero, Solid character of membrane ceramides: a surface rheology study of their mixtures with sphingomyelin, Biophys. J. 101 (2011) 2721–2730.

[28] J.T. Petkov, K.D. Danov, N.D. Denkov, Precise method for measuring the shear surface viscosity of surfactant monolayers, Langmuir 12 (1996) 2650–2653.
[29] B. Caruso, A. Mangiarotti, N. Wilke, Stiffness of lipid monolayers with phase coexistence, Langmuir 29 (2013) 10807–10816.
[30] N.R. Pallas, B.A. Petica, Liquid-expanded to liquid-condensed transitions in lipid monolayers at the air/water interface, Langmuir 1 (1985) 509–513.
[31] T. Gutberlet, D. Vollhardt, Thermally induced domain growth in fatty acid ester monolayer, J. Colloid Interface Sci. 173 (2013) 429–435.
[32] D. Andelman, F. Brochard, J.F. Joanny, Phase transition in langmuir monolayers of polar molecules, J. Chem. Phys. 86 (1987) 3673–3681.
[33] C.M. Rosetti, N. Wilke, B. Maggio, Thermodynamic distribution functions associated to the isothermal phase transition in Langmuir monolayers, Chem. Phys. Lett. 422 (2006) 240–245.
[34] J.N. Israelachvili, Self assembled in two dimensions: surface micelles and domain formation in monolayers, Langmuir 10 (1994) 3781.
[35] V.B. Fainerman, D. Vollhardt, Phase transition in Langmuir monolayers, Colloids Surf. A 176 (2002) 124.
[36] L.R. Arriaga, I. Lopez-Montero, J. Ignes-Mullol, F. Monroy, Domain-growth kinetic origin of nonhorizontal phase coexistence plateaux in langmuir monolayers: compression rigidity of a Raft-like lipid distribution, J. Phys. Chem. B 114 (2010) 4509–4520.
[37] E. Ruckenstein, B. Li, Surface equation of state for insoluble surfactant monolayers at the air/water Interface, J. Phys. Chem. B 102 (1998) 981–989.
[38] C. Lheveder, J. Meunier, S. Henon, Brewster angle microscopy, in: A. Baszkin, W. Norde (Eds.), Physical Chemistry of Biological Interfaces, Marcel Dekker Inc., NY, 2000.
[39] J.G. Petrov, T. Pfohl, H. Mohwald, Ellipsometric chain length dependence of fatty acid Langmuir monolayers. A heads-and-tails model, J. Phys. Chem. B 103 (1999) 3417–3424.
[40] F. Vega Mercado, B. Maggio, N. Wilke, Phase diagram of mixed monolayers of stearic acid and dimyristoylphosphatidylcholine. Effect of the acid ionization, Chem. Phys. Lipids 164 (2011) 386–392.
[41] D. Ducharme, J.J. Max, C. Salesse, R.M. Leblanc, Ellipsometric study of the physical states of phosphatidylcholine at the air-water interface, J. Phys. Chem. 94 (1990) 1925–1932.
[42] R.J. Clarke, The dipole potential of phospholipid membranes and methods for its detection, Adv. Colloid Interface Sci. 90 (2001) 263–281.
[43] J.M. Smaby, H.L. Brockman, Surface dipole moments of lipids at the argon-water interface. Similarities among glycerol-ester-based lipids, Biophys. J. 58 (1990) 195–204.
[44] D.M. Taylor, Developments in the theoretical modelling and experimental measurement of the surface potential of condensed monolayers, Adv. Colloid Interface Sci. 87 (2000) 183–203.
[45] G. Vogel, D. Mobius, Local surface potentials and electric dipole moments of lipid monolayers: contributions of the water/lipid and the lipid/air interfaces, J. Colloid Interface Sci. 126 (1988) 408–420.
[46] K. Gawrisch, D. Ruston, J. Zimmerberg, V.A. Parsegian, R.P. Rand, N. Fuller, Membrane dipole potentials, hydration forces, and the ordering of water at membrane surfaces, Biophys. J. 61 (1992) 1213–1223.
[47] A. Miller, C. Helm, H. Möhwald, The colloidal nature of phospholipid monolayers, J. Geophys. Res. 48 (1987) 693–701.
[48] P.T. Frangopol, D. Ilescu, Interactions of some local anesthetics and alcohols with membranes, Colloids Surf. B Biointerfaces 22 (2001) 3–22.

[49] M.A. Bos, T. Nylander, Interaction between â-lactoglobulin and phospholipids at the air/water interface, Langmuir 12 (1996) 2792–2797.
[50] S. Deshayes, T. Plenat, G. Aldrian-Herrada, G. Divita, G.C. Le, F. Heitz, Primary amphipathic cell-penetrating peptides: structural requirements and interactions with model membranes, Biochemistry 43 (2004) 7698–7706.
[51] R. Miller, V.B. Fainerman, A.V. Makievski, J. Kragel, D.O. Grigoriev, V.N. Kazakov, O.V. Sinyachenko, Dynamics of protein and mixed protein/surfactant adsorption layers at the water/fluid interface, Adv. Colloid Interface Sci. 86 (2000) 39–82.
[52] C. Larios, J. Minones Jr., I. Haro, M.A. Alsina, M.A. Busquets, J.M. Trillo, Study of adsorption and penetration of E2(279-298) peptide into Langmuir phospholipid monolayers, J. Phys. Chem. B 110 (2006) 23292–23299.
[53] M. Eeman, A. Berquand, Y.F. Dufrene, M. Paquot, S. Dufour, M. Deleu, Penetration of surfactin into phospholipid monolayers: nanoscale interfacial organization, Langmuir 22 (2006) 11337–11345.
[54] R. Volinsky, S. Kolusheva, A. Berman, R. Jelinek, Investigations of antimicrobial peptides in planar film systems, Biochim. Biophys. Acta 1758 (2006) 1393–1407.
[55] R. Verger, F. Pattus, Lipid-protein interactions in monolayers, Chem. Phys. Lipids 30 (1983) 227.
[56] R. Maget-Dana, The monolayer technique: a potent tool for studying the interfacial properties of antimicrobial and membrane-lytic peptides and their interactions with lipid membranes, Biochim. Biophys. Acta 1462 (1999) 109–140.
[57] M. Mottola, N. Wilke, L. Benedini, R.G. Oliveira, M.L. Fanani, Ascorbyl palmitate interaction with phospholipid monolayers: electrostatic and rheological preponderancy, Biochim. Biophys. Acta 1828 (2013) 2496–2505.
[58] G. Barnes, I. Gentle, Interfacial Science, Oxford University Press, Oxford, 2005.
[59] D. Vollhardt, V.B. Fainerman, Characterisation of phase transition in adsorbed monolayers at the air/water interface, Adv. Colloid Interface Sci. 154 (2010) 1–19.
[60] F.D. Evans, H. Wennerstrom, The Colloid Domain, Wiley-VCH, USA, 1999.
[61] L. Benedini, M.L. Fanani, B. Maggio, N. Wilke, P. Messina, S. Palma, P. Schulz, Surface phase behavior and domain topography of ascorbyl palmitate monolayers, Langmuir 27 (2011) 10914–10919.
[62] R.A. Bockmann, A. Hac, T. Heimburg, H. Grubmuller, Effect of sodium chloride on a lipid bilayer, Biophys. J. 85 (2003) 1647–1655.
[63] M. Yi, H. Nymeyer, H.X. Zhou, Test of the Gouy-Chapman theory for a charged lipid membrane against explicit-solvent molecular dynamics simulations, Phys. Rev. Lett. 101 (2008) 038103.
[64] K. Simons, W.L. Vaz, Model systems, lipid rafts, and cell membranes, Annu. Rev. Biophys. Biomol. Struct. 33 (2004) 269–295.
[65] C.D. Blanchette, W.C. Lin, C.A. Orme, T.V. Ratto, M.L. Longo, Using nucleation rates to determine the interfacial line tension of symmetric and asymmetric lipid bilayer domains, Langmuir 23 (2007) 5875–5877.
[66] Th.M. Fischer, M. Losche, Pattern formation in langmuir monolayers due to long-range electrostatic interactions, Lect. Notes Phys. 634 (2004) 383–394.
[67] U. Bernchou, J.H. Ipsen, A.C. Simonsen, Growth of solid domains in model membranes: quantitative image analysis reveals a strong correlation between domain shape and spatial position, J. Phys. Chem. B 113 (2009) 7170–7177.
[68] F. Vega Mercado, B. Maggio, N. Wilke, Modulation of the domain topography of biphasic monolayers of stearic acid and dimyristoyl phosphatidylcholine, Chem. Phys. Lipids 165 (2012) 232–237.
[69] A. Miller, H. Möhwald, Collecting two-dimensional phospholipid crystals in inhomogeneous electric fields, Europhys. Lett. 2 (1986) 67–74.

[70] N. Wilke, S.A. Dassie, E.P. Leiva, B. Maggio, Externally applied electric fields on immiscible lipid monolayers: repulsion between condensed domains precludes domain migration, Langmuir 22 (2006) 9664–9670.
[71] N. Wilke, B. Maggio, Effect of externally applied electrostatic fields on the surface topography of ceramide-enriched domains in mixed monolayers with sphingomyelin, Biophys. Chem. 122 (2006) 36–42.
[72] P.I. Kuzmin, S.A. Akimov, Y.A. Chizmadzhev, J. Zimmerberg, F.S. Cohen, Line tension and interaction energies of membrane rafts calculated from lipid splay and tilt, Biophys. J. 88 (2005) 1120–1133.
[73] S.A. Akimov, P.I. Kuzmin, J. Zimmerberg, F.S. Cohen, Y.A. Chizmadzhev, An elastic theory for line tension at a boundary separating two lipid monolayer regions of different thickness, J. Electroanal. Chem. 564 (2004) 13–18.
[74] S.A. Akimov, P.I. Kuzmin, J. Zimmerberg, F.S. Cohen, Lateral tension increases the line tension between two domains in a lipid bilayer membrane, Phys. Rev. E Stat. Nonlin. Soft Matter Phys. 75 (2007) 011919.
[75] A.J. Garcia-Saez, S. Chiantia, P. Schwille, Effect of line tension on the lateral organization of lipid membranes, J. Biol. Chem. 282 (2007) 33537–33544.
[76] M.L. Fanani, B. Maggio, Liquid-liquid domain miscibility driven by composition and domain thickness mismatch in ternary lipid monolayers, J. Phys. Chem. B 115 (2011) 41–49.
[77] D.W. Lee, Y. Min, P. Dhar, A. Ramachandran, J.N. Israelachvili, J.A. Zasadzinski, Relating domain size distribution to line tension and molecular dipole density in model cytoplasmic myelin lipid monolayers, Proc. Natl. Acad. Sci. U.S.A 108 (2011) 9425–9430.
[78] I. Sriram, D.K. Schwartz, Line tension between coexisting phases in monolayers and bilayers of amphiphilic molecules, Surface Sci. Rep. 67 (2012) 143–159.
[79] R. De Koker, H.M. McConnell, Circle to dogbone: shapes and shape transitions of lipid monolayer domains, J. Phys. Chem. B 97 (1993) 13419–13424.
[80] J. Lauger, Ch.R. Robertson, C.W. Frank, G.G. Fuller, Deformation and relaxation processes of mono- and bilayer domains of liquid crystalline langmuir films on water, Langmuir 12 (1996) 5630–5635.
[81] J.R. Wintersmith, L. Zou, A.J. Bernoff, J.C. Alexander, J.A. Mann Jr., E.E. Kooijman, E.K. Mann, Determination of interphase line tension in Langmuir films, Phys. Rev. E Stat. Nonlin. Soft Matter Phys. 75 (2007) 061605.
[82] S. Wurlitzer, P. Steffen, T.M. Fischer, Line tension of Langmuir monolayer phase boundaries determined with optical tweezers, J. Chem. Phys. 112 (2000) 5915–5918.
[83] A.A. Bischof, N. Wilke, Molecular determinants for the line tension of coexisting liquid phases in monolayers, Chem. Phys. Lipids 165 (2012) 737–744.
[84] A.R. Honerkamp-Smith, P. Cicuta, M.D. Collins, S.L. Veatch, N.M. den, M. Schick, S.L. Keller, Line tensions, correlation lengths, and critical exponents in lipid membranes near critical points, Biophys. J. 95 (2008) 236–246.
[85] M. Seul, Dynamics of domain shape relaxation in langmuir films, J. Phys. Chem. 97 (1993) 2941–2945.
[86] B.L. Stottrup, A.H. Nguyen, E. Tuzel, Taking another look with fluorescence microscopy: image processing techniques in Langmuir monolayers for the twenty-first century, Biochim. Biophys. Acta 1798 (2010) 1289–1300.
[87] A. Tian, C. Johnson, W. Wang, T. Baumgart, Line tension at fluid membrane domain boundaries measured by micropipette aspiration, Phys. Rev. Lett. 98 (2007) 208102.
[88] C.D. Blanchette, W.C. Lin, C.A. Orme, T.V. Ratto, M.L. Longo, Domain nucleation rates and interfacial line tensions in supported bilayers of ternary mixtures containing galactosylceramide, Biophys. J. 94 (2008) 2691–2697.

[89] C.D. Blanchette, C.A. Orme, T.V. Ratto, M.L. Longo, Quantifying growth of symmetric and asymmetric lipid bilayer domains, Langmuir 24 (2008) 1219–1224.
[90] P. Dhar, E. Eck, J.N. Israelachvili, D.W. Lee, Y. Min, A. Ramachandran, A.J. Waring, J.A. Zasadzinski, Lipid-protein interactions alter line tensions and domain size distributions in lung surfactant monolayers, Biophys. J. 102 (2012) 56–65.
[91] H.M. McConnell, Equilibration rates in lipid monolayers, Proc. Natl. Acad. Sci. U.S.A 93 (1996) 15001–15003.
[92] L.V. Schafer, S.J. Marrink, Partitioning of lipids at domain boundaries in model membranes, Biophys. J. 99 (2010) L91–L93.
[93] S. Trabelsi, S. Zhang, T.R. Lee, D.K. Schwartz, Linactants: surfactant analogues in two dimensions, Phys. Rev. Lett. 100 (2008) 037802.
[94] S. Trabelsi, Z. Zhang, S. Zhang, T.R. Lee, D.K. Schwartz, Correlating linactant efficiency and self-assembly: structural basis of line activity in molecular monolayers, Langmuir 25 (2009) 8056–8061.
[95] O. Szekely, Y. Schilt, A. Steiner, U. Raviv, Regulating the size and stabilization of lipid raft-like domains and using calcium ions as their probe, Langmuir 27 (2011) 14767–14775.
[96] M. Karttunen, M.P. Haataja, M. Saily, I. Vattulainen, J.M. Holopainen, Lipid domain morphologies in phosphatidylcholine-ceramide monolayers, Langmuir 25 (2009) 4595–4600.
[97] C.W. McConlogue, T.K. Vanderlick, Molecular determinants of lipid domain shape, Langmuir 15 (1999) 234–237.
[98] D.J. Benvegnu, H.M. McConnell, Surface dipole densities in lipid monolayers, J. Phys. Chem. 97 (1993) 6686–6691.
[99] P.A. Rice, H.M. McConnell, Critical shape transitions of monolayer lipid domains, Proc. Natl. Acad. Sci. U.S.A 86 (1989) 6445–6448.
[100] D. Gallez, H.M. McConnell, Coupling of size and shape equilibration in lipid monolayer domains, J. Phys. Chem. B 104 (2000) 1657–1662.
[101] H.A. Stone, H.M. McConnell, Hydrodynamics of quantized shape transitions of lipid domains, Proc. R. Soc. Lond. A 448 (1995) 97–111.
[102] S. Wurlitzer, Th.M. Fischer, H. Schmiedel, Equilibrium size of circular domains in Langmuir monolayers, J. Chem. Phys. 116 (2002) 10877–10881.
[103] M.L. Fanani, T.L. De, S. Hartel, J. Jara, B. Maggio, Sphingomyelinase-induced domain shape relaxation driven by out-of-equilibrium changes of composition, Biophys. J. 96 (2009) 67–76.
[104] P. Kruger, M. Losche, Molecular chirality and domain shapes in lipid monolayers on aqueous surfaces, Phys. Rev. E Stat. Phys. Plasmas Fluids Relat. Interdiscip. Topics 62 (2000) 7031–7043.
[105] B.M. Discher, K.M. Maloney, D.W. Grainger, S.B. Hall, Effect of neutral lipids on coexisting phases in monolayers of pulmonary surfactant, Biophys. Chem. 101–102 (2002) 333–345.
[106] C. Yuan, L.J. Johnston, Distribution of ganglioside GM1 in L-dipalmitoylphosphatidylcholine/cholesterol monolayers: a model for lipid rafts, Biophys. J. 79 (2000) 2768–2781.
[107] M.M. Hossain, T. Kato, Line tension induced instability of condensed domains formed in adsorbed monolayers at the air-water interface, Langmuir 16 (2000) 10175–10183.
[108] N. Krasteva, D. Vollhardt, Morphology and phase behaviour of monoglyceride monolayers on aqueous sugar substrates, Colloids Surf. A Physicochem. Eng. Asp. 171 (2000) 49–57.
[109] W.J. Foster Jr., P.A. Janmey, The distribution of polyphosphoinositides in lipid films, Biophys. Chem. 91 (2001) 211–218.

[110] A. Cevers, P.A. Janmey, Shape instabilityes in charged lipid domains, J. Phys. Chem. B 106 (2002) 12351–12353.
[111] S.M. Loverde, C.M. Olvera de la, Asymmetric charge patterning on surfaces and interfaces: formation of hexagonal domains, J. Chem. Phys. 127 (2007) 164707.
[112] N. Nandi, D. Vollhardt, Effect of molecular chirality on the morphology of biomimetic langmuir monolayers, Chem. Rev. 103 (2003) 4033–4076.
[113] P. Scholtysek, Z. Li, J. Kressler, A. Blume, Interactions of DPPC with semitelechelic poly(glycerol methacrylate)s with perfluoroalkyl end groups, Langmuir 28 (2012) 15651–15662.
[114] R. Bruinsma, F. Rondelez, A. Levine, Flow-controlled growth in Langmuir monolayers, Eur. Phys. J. E 6 (2001) 191–200.
[115] A. Gutierrez-Campos, G. Az-Leines, R. Castillo, Domain growth, pattern formation, and morphology transitions in Langmuir monolayers. A new growth instability, J. Phys. Chem. B 114 (2010) 5034–5046.
[116] P.F. Almeida, W.L. Vaz, T.E. Thompson, Lateral diffusion and percolation in two-phase, two-component lipid bilayers. Topology of the solid-phase domains in-plane and across the lipid bilayer, Biochemistry 31 (1992) 7198–7210.
[117] T.V. Ratto, M.L. Longo, Obstructed diffusion in phase-separated supported lipid bilayers: a combined atomic force microscopy and fluorescence recovery after photobleaching approach, Biophys. J. 83 (2002) 3380–3392.
[118] M. Forstner, D. Martin, F. Rückerl, J. Käs, C. Selle, Attractive membrane domains control lateral diffusion, Phys. Rev. E. 77 (2008), 051906-1-051906-7.
[119] P. Nassoy, W.R. Birch, D. Andelman, F. Rondelez, Hydrodynamic mapping of two-dimensional electric fields in monolayers, Phys. Rev. Lett. 76 (1996) 455–458.
[120] P. Cicuta, S.L. Keller, S.L. Veatch, Diffusion of liquid domains in lipid bilayer membranes, J. Phys. Chem. B 111 (2007) 3328–3331.
[121] N. Wilke, B. Maggio, The influence of domain crowding on the lateral diffusion of ceramide-enriched domains in a sphingomyelin monolayer, J. Phys. Chem. B 113 (2009) 12844–12851.
[122] B. Caruso, M.A. Villarreal, L. Reinaudi, N. Wilke, Inter-domain interactions in charged lipid monolayers, Langmuir 118 (2014) 519–529.
[123] D. Hughes, B. Pailthorpe, L. White, The translational and rotational drag on a cylinder moving in a membrane, J. Fluid Mech. 110 (1981) 349–372.
[124] M. Sickert, F. Rondelez, H.A. Stone, Single-particle Brownian dynamics for characterizing the rheology of fluid Langmuir monolayer, Europhys Lett. 79 (2007) 66005–66011.
[125] F. Ruckerl, J.A. Kas, C. Selle, Diffusion of nanoparticles in monolayers is modulated by domain size, Langmuir 24 (2008) 3365–3369.
[126] J. Ding, H.E. Warriner, J.A. Zasadzinski, Viscosity of two-dimensional suspensions, Phys. Rev. Lett. 88 (2002) 168102.
[127] S. Hartel, M.L. Fanani, B. Maggio, Shape transitions and lattice structuring of ceramide-enriched domains generated by sphingomyelinase in lipid monolayers, Biophys. J. 88 (2005) 287–304.
[128] A.C. Simonsen, L.A. Bagatolli, Structure of spin-coated lipid films and domain formation in supported membranes formed by hydration, Langmuir 20 (2004) 9720–9728.
[129] W.C. Lin, C.D. Blanchette, T.V. Ratto, M.L. Longo, Lipid asymmetry in DLPC/DSPC-supported lipid bilayers: a combined AFM and fluorescence microscopy study, Biophys. J. 90 (2006) 228–237.
[130] M. Seul, M.J. Sammon, Preparation of surfactant multilayer films on solid substrates by deposition from organic solution, Thin Solid Films 185 (1990) 287–305.

[131] J. Sanchez, A. Badia, Atomic force microscopy studies of lateral phase separation in mixed monolayer of dipalmitoylphosphatidylcholine and dilauroylphosphatodylcholine, Thin Solid Films 440 (2003) 223–239.
[132] R.P. Richter, A.R. Brisson, Following the formation of supported lipid bilayers on mica: a study combining AFM, QCM-D, and ellipsometry, Biophys. J. 88 (2005) 3422–3433.
[133] M. Golabek, M. Jurak, L. Holysz, E. Chibowski, The energetic and topography changes of mixed lipid bilayers deposited on glass, Colloids Surf. A 391 (2011) 150–157.
[134] H.M. Seeger, C.A. Di, A. Alessandrini, P. Facci, Supported lipid bilayers on mica and silicon oxide: comparison of the main phase transition behavior, J. Phys. Chem. B 114 (2010) 8926–8933.
[135] B.L. Stottrup, S.L. Veatch, S.L. Keller, Nonequilibrium behavior in supported lipid membranes containing cholesterol, Biophys. J. 86 (2004) 2942–2950.
[136] B.L. Stottrup, D.S. Stevens, S.L. Keller, Miscibility of ternary mixtures of phospholipids and cholesterol in monolayers, and application to bilayer systems, Biophys. J. 88 (2005) 269–276.
[137] C.B. Babayco, T. Sennur, A.M. Smith, B. Sanii, D. Land, A. Parikh, A comparison of lateral diffusion in supported lipid monolayers and bilayers, Soft Matter 6 (2010) 5877–5881.
[138] F. Tokumasu, A.J. Jin, G.W. Feigenson, J.A. Dvorak, Nanoscopic lipid domain dynamics revealed by atomic force microscopy, Biophys. J. 84 (2003) 2609–2618.
[139] F. Tokumasu, A.J. Jin, J.A. Dvorak, Lipid membrane phase behaviour elucidated in real time by controlled environment atomic force microscopy, J. Electron Microsc. (Tokyo) 51 (2002) 1–9.
[140] V. Kiessling, C. Wan, L.K. Tamm, Domain coupling in asymmetric lipid bilayers, Biochim. Biophys. Acta 1788 (2009) 64–71.
[141] S.L. Veatch, S.L. Keller, Seeing spots: complex phase behavior in simple membranes, Biochim. Biophys. Acta 1746 (2005) 172–185.
[142] S.L. Veatch, S.L. Keller, Organization in lipid membranes containing cholesterol, Phys. Rev. Lett. 89 (2002) 268101.
[143] A. Mangiarotti, B. Caruso, N. Wilke, Phase coexistence in films composed of DLPC and DPPC: a comparison between different model membrane systems, Biochim. Biophys. Acta. Biomembr. 1838 (2014) 1823–1831.
[144] G. Gopalakrishnan, I. Rouiller, D.R. Colman, R.B. Lennox, Supported bilayers formed from different phospholipids on spherical silica substrates, Langmuir 25 (2009) 5455–5458.
[145] A.L. Troutier, C. Ladaviere, An overview of lipid membrane supported by colloidal particles, Adv. Colloid Interface Sci. 133 (2007) 1–21.
[146] C. Naumann, T. Brumm, T.M. Bayerl, Phase transition behavior of single phosphatidylcholine bilayers on a solid spherical support studied by DSC, NMR and FT-IR, Biophys. J. 63 (1992) 1314–1319.
[147] A. Charrier, F. Thibaudau, Main phase transitions in supported lipid single-bilayer, Biophys. J. 89 (2005) 1094–1101.
[148] R.A. Demel, W.S. Geurts van Kessel, R.F. Zwaal, B. Roelofsen, L.L. van Deenen, Relation between various phospholipase actions on human red cell membranes and the interfacial phospholipid pressure in monolayers, Biochim. Biophys. Acta 406 (1975) 97–107.
[149] D. Marsh, Lateral pressure in membranes, Biochim. Biophys. Acta 1286 (1996) 183–223.
[150] M.C. Phillips, D.E. Graham, H. Hauser, Lateral compressibility and penetration into phospholipid monolayers and bilayer membranes, Nature 254 (1975) 154–156.

[151] N. Albon, J.F. Baret, Comparison and correlation between the properties of lipid molecules in crystals, bilayer dispersions in water and monolayers on a water surface, J. Colloid Interface Sci. 92 (1983) 545–560.
[152] B. Maggio, G.D. Fidelio, F.A. Cumar, R.K. Yu, Molecular interactions and thermotropic behavior of glycosphingolipids in model membrane systems, Chem. Phys. Lipids 42 (1986) 49–63.
[153] B. Maggio, The surface behavior of glycosphingolipids in biomembranes: a new frontier of molecular ecology, Prog. Biophys. Mol. Biol. 62 (1994) 55–117.
[154] J. Liu, S. Qi, J.T. Groves, A.K. Chakraborty, Phase segregation on different length scales in a model cell membrane system, J. Phys. Chem. B 109 (2005) 19960–19969.
[155] R. Parthasarathy, J.T. Groves, Curvature and spatial organization in biological membranes, Soft Matter 3 (2007) 24–33.
[156] M. Benes, D. Billy, A. Benda, H. Speijer, M. Hof, W.T. Hermens, Surface-dependent transitions during self-assembly of phospholipid membranes on mica, silica, and glass, Langmuir 20 (2004) 10129–10137.
[157] H.P. Wacklin, Composition and asymmetry in supported membranes formed by vesicle fusion, Langmuir 27 (2011) 7698–7707.
[158] M. Przybylo, J. Sykora, J. Humpolickova, A. Benda, A. Zan, M. Hof, Lipid diffusion in giant unilamellar vesicles is more than 2 times faster than in supported phospholipid bilayers under identical conditions, Langmuir 22 (2006) 9096–9099.